Mesh adaption strategies for steady shallow water flow.

M. Marrocu[1] & D. Ambrosi[2]

1 - Centro di Ricerca, Sviluppo e Studi Superiori in Sardegna (CRS4), Cagliari, Italy; email: marino@crs4.it

2 - Dipartimento di Matematica, Politecnico di Torino, corso Duca degli Abruzzi 24, 10129 Torino, Italy

Abstract

The use of unstructured grids for the numerical approximation of partial differential equations of applied mathematics has the great appeal of enabling mesh adaption based on suitable error indicators of the accuracy of the solution, refining the mesh where the numerical error is large and coarsening it where the error is small. In this way it is then possible to optimize the quality of the solution for a given computational effort. We deal here with mesh adaption applied to shallow water flow. The shallow water equations are numerically approximated by a standard Galerkin finite element method, using linear elements for the elevation field and quadratic elements for the unit-width discharge field. The advancing-in-time scheme used is of fractional step type. The standard mesh refinement technique is used; movement and elimination of nodes of the initial triangulation is not allowed. Two empirical error indicators are proposed and applied here to to an ideal case of steady flow. The numerical tests show that mesh adaption is a very reliable tool for numerical simulation of shallow water steady flow. Any of the used error indicators produce numerical results that are strongly improved with respect to a uniform mesh, with only a minor increase in the computational effort.

1 Introduction

The capability to handle problems characterized by computational domains with complex boundaries, but above all the possibility to

refine the computational mesh where needed, are some of the advantages that can be achieved using unstructured grids for the discretization of partial differential equations. In particular, if some suitable indicator of the accuracy of the solution is used, the quality of the computed solution can be optimized.
Mesh adaption techniques have already been extensively used in several fields of computational physics, but adaptivity has not yet much explored in the framework of free surface hydrostatic flow. To our knowledge only a very recent paper [5] compares and discusses the use of high order polynomial basis (p adaption) for the discretization of the shallow water equations versus local mesh refinement, where the order of the polynomial approximation is kept unchanged (h adaption).
We apply mesh adaption strategies to the discretization of the so called shallow water equations, and propose two empirical error indicators to drive the adaption procedure. Numerical results obtained applying this procedure to a test case of steady flow are then discussed.

2 The shallow water equations and the numerical scheme

The shallow water equations may be written in conservative differential form as

$$\frac{\partial \mathbf{q}}{\partial t}+\nabla\cdot(\mathbf{q}\otimes\mathbf{q}/H)-\nabla\cdot(\mu\nabla\mathbf{q})+gH\nabla\xi = -g\frac{\mathbf{q}|\mathbf{q}|}{H^2H^{1/3}K^2}-2\Omega\times\mathbf{q} \quad (1)$$

$$\frac{\partial \xi}{\partial t}+\nabla\cdot\mathbf{q}=0 \quad (2)$$

where $\mathbf{q}(x,y,t)=(q_x,q_y)^T$ is the unit-width discharge, ξ is the elevation over a reference plane, H is the total depth of the water, μ is the dispersion coefficient, g is the gravity acceleration, Ω is the angular velocity of the earth and K is the Strickler coefficient. The numerical scheme used to approximate the shallow water equations (1-2) is a finite element scheme of fractional step type.
The main idea of the time advancing scheme is to split the equations at every time step, in order to decouple the different physical contributions: convection, propagation, diffusion and bottom friction.The

spatial discretization of the equations is based on a standard Galerkin finite element method; the basic theory of the Galerkin approach may be found, for example, in [2] and [6]. An important aspect of the spatial discretization is that two different spaces of representation have been used for the unknowns: the elevation is interpolated by piecewise linear (P1) functions, whilst the unit-width discharge is interpolated by piecewise quadratic (P2) functions. The choice of these interpolation spaces eliminates the spurious oscillations that arise in the elevation field when a P1-P1 representation is used inside a scheme that involves an elliptic equation. The interested reader can find a more detailed discussion of the all integration scheme procedures in [1].

3 Error indicators and adaption technique

For linear elliptic problems it is possible to estimate rigorously the numerical error in terms of the second derivative of the solution. Let u be the exact solution of the Poisson problem in weak form: $(\nabla u, \nabla v) = (b, v)$, for all v belonging to a suitable space and where $(\, , \,)$ indicates the usual internal product in L^2, and let u_h be the solution of the discrete equation $(\nabla u_h, \nabla v_h) = (b, v_h)$, where $\{v_h\}$ is a finite subset of test functions. Then, given a triangulation with maximum side length h, it can be shown [2] that the distance between the exact and the computed solution linear in H^1 is bounded as follows:

$$\| \nabla(u - u_h) \|_{L^\infty} \leq C h^2 \max_{\Omega} \max_{ij} | H \frac{\partial u}{\partial x_i \partial x_j} | \tag{3}$$

where Ω is the computational domain. As the computational kernel of the numerical scheme described in Section 2 is an elliptic equation for the elevation of the water, a possible approach in the refining–coarsening stage is to use the estimate (3), where the right hand side has to be calculated using the computed solution u_h. Let the unknown $\xi(\mathbf{x}) = \sum_k \phi_k(\mathbf{x})\xi_k$, be represented using the standard finite elements linear basis $\{\phi_k\}$, the error estimate (3) suggests, then, to define the following non–dimensional error indicator:

$$\epsilon_{1,m} = \frac{H_m}{\xi_m} \max_{ij} | \sum_k \xi_k \int_\Omega \frac{\partial \phi_k}{\partial x_i} \frac{\partial \phi_m}{\partial x_j} \, d\Omega |, \tag{4}$$

where the water elevation is assumed to never vanish in the computational domain.

An important feature that a numerical scheme for shallow water flow should possess is mass conservation. This property is accomplished by the scheme described above in a weak sense, as the discrete equations are obtained from the continuity equations (1), and are then consistent with it. However, the finite element scheme illustrated above does not ensure mass conservation in a *finite–volume cell–centered* sense: the mass variation inside a triangle during a time step is not exactly equal to the flux through the edges of the triangle itself. This consideration suggests to use the check of local mass balance as an error indicator for the present scheme. We define then

$$\epsilon_{2,e} = |\frac{1}{\Delta t}\int_e (\xi^n - \xi^{n-1}) d\Omega + \oint_e \mathbf{q}^n \cdot d\Gamma| \tag{5}$$

where Γ is the contour of the e-th element and $\epsilon_{2,e}$ is the mass deficit in the e-th element.

The error estimators proposed can be used to identify a set of elements of the mesh to be refined (or coarsened). Several techniques can then be used to this aim, such as repositioning the mesh (r-methods), enrichment of the mesh (h-methods) or re-meshing (m-methods). The choice of the most suitable mesh adaption procedure depends on the problem at hand [3].

In the present paper we apply an h-method. Teh main reason for this choice is that h-methods keep the information on the original grid unchanged. When a new node is added in the middle of an edge, batimetry, velocity, and water elevation in it are obtained by interpolating the values in the element. In this way the original values of the batimetry and of the physical unknowns in the initial mesh are never abandoned and the degradation of the solution by interpolation is minimized.

The technique used to subdivide an element is the so called *standard refinement* within which an element is split into four similar elements joining midpoints of each edge [4]. When all the elements to be refined are split in a standard way, the surrounding triangles may have a new node in the midpoint of an edge. These elements are refined joining the new node to the opposite vertex of the triangle (*green refinement*). We have used a strategy which minimizes the number of *green* elements, as these elements deteriorate the quality of the initial mesh.

In practice we started with a quite coarse mesh, and refined it until a determined number of nodes is reached.

4 Numerical results and conclusions

To investigate numerically the performance of the mesh adaption strategy outlined above, we have chosen a test case involving several characteristic features of shallow water flow.

In Fig.1.a we show the geometry of the channel and the initial computational mesh used for the present calculations. The test is designed to collect in a sketchy fashion a number of typical situations that occur in river flow. The main channel is 2 kilometers long and 100 meters large (see also Fig.2), it has an abrupt enlargement that doubles its width, a smaller inflowing branch, and a square island in the middle. In the initial part, the bottom of the channel has a constant depth of 3 meters, in the final part behind the small island the depth has a jump and rapidly becomes 6 meters. The inflow boundary conditions of the main channel and of the secondary channel are 300 and 100 cubic meters per second, respectively. At the outflow, a constant water elevation is imposed.

The initial computational mesh is intentionally quite coarse, being composed by 120 nodes only (see fig.1.a). The simulation performed on this initial grid (solution u_0), has been made 300 time steps long of 50s each one. The stationary state so obtained does not reveal recirculation neither behind the abrupt enlargement nor behind the island, that in fact do exist, and the shear near the right corner of the inflow of the smaller channel where the two streams collide is poorly described. These are also zones where the bigger errors are located (see Fig.2).

The adaption procedure driven by both error indicators has been applied refining the initial grid adaptively every 76 time steps for three times. The threshold errors have been chosen in such way that the final meshes are composed of about 370 nodes (see last column of Table 1).

Both error indicators lead to meshes refined in the regions of interest (see Fig.1.b): near the left and the right corner of the inflow of the smaller channel, near the channel enlargement, in the region around the island, and in correspondence of the batimetry jump.

To get a quantitative evaluation of the quality of the adaptively refined meshes, a numerical simulation has been run on a grid obtained refining three times all the elements of the background grid up to a final number of elements which is 64 times the initial one. The numerical solution computed on the finest grid is then taken as the

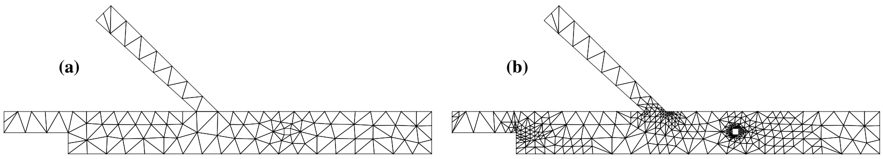

Figure 1: Background (a) and refined grid (b) obtained using the error indicators ϵ_2; the mesh obtained using the error indicator ϵ_1, not shown here, is very similar to this last.

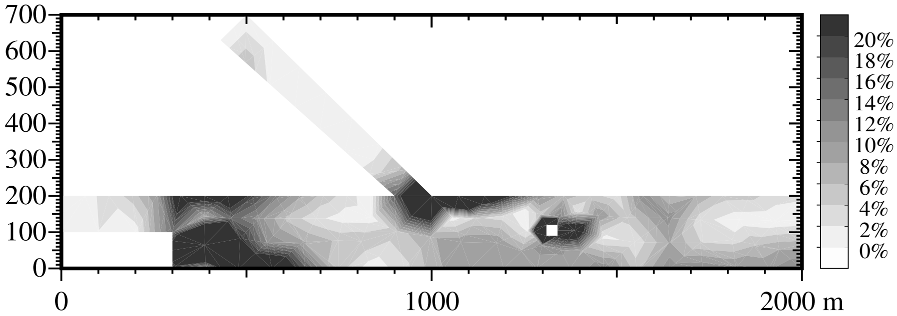

Figure 2: Local percentage error of discharge field η_i^q of the u_0 solution, obtained using the background mesh.

reference one, and the numerical percentage error is evaluated comparing the water elevation and discharge computed on the finest mesh and the values computed on the adaptively refined meshes

$$\eta_i^\xi = \frac{|\xi_{3,i} - \xi_i|}{\xi_{3,i}}, \qquad \eta_i^q = \frac{|q_{3,i} - q_i|}{\overline{q_3}}, \tag{6}$$

where $\xi_{3,i}$, $\hat{q}_{3,i}$, is the reference solution in the i-th node computed on the finest grid. In the denominator of the discharge error the mean value of the discharge ($\overline{q}_3$) is used so as not to overestimate the contribution due to the stagnation points.

Generally speaking, the plots of η_i^ξ and η_i^q (not shown) show that, for the two adapted solutions (u_{ϵ_1}, u_{ϵ_1}), the biggest local residual error is strongly confined around the island, that is the region mostly refined of the adapted meshes. The maximum residual error in the water elevation is about 5% and that of the magnitude of the discharge is about 10%. In any case in the great part of the domain the errors for the elevation are lower than 1%, and only a bit greater for the

solution	$\overline{\eta^\xi}(\%)$	$\overline{\eta^q}(\%)$	NV1
u_0	7.0	10.2	120
u_1	6.0	5.7	403
u_2	1.6	2.2	1458
u_{ϵ_1}	2.3	2.4	361
u_{ϵ_2}	1.1	2.0	375

Table 1: Average percentage errors of the computed solutions and number of P1 nodes (NV1).

discharge.

A global measure of the errors can be obtained averaging the errors defined in 6. Results are in Table 1. The mean percentage errors of the two adapted solutions are much lower than those of the u_0 solution ($\overline{\eta^\xi} = 7\%$, $\overline{\eta^q} = 10.2\%$). The errors of the u_{ϵ_2} solution ($\overline{\eta^\xi} = 1.1\%$, $\overline{\eta^q} = 2.0\%$) are a little lower than those of the u_{ϵ_1} solution ($\overline{\eta^\xi} = 2.3\%$, $\overline{\eta^q} = 2.4\%$) but this could be related to the different number of nodes in the two final meshes (see last column of the table).

The rate of convergence of the numerical solution, to the exact one by refining globally the grid, has been obtained comparing the solution u_0 and the reference solution with those obtained refining the background mesh uniformly one and two times (u_1 and u_2 solutions). Looking at the global percentage errors in the Table 1, it appears that the solution on the background grid (u_0) is poor and differs not much with respect to that on the grid uniformly refined one time (u_1). Errors of the u_2 solution are instead much smaller indicating that the solution on the finest grid is converging.

The more striking result that can be deduced by the numbers in the table is that the adapted solution ($\sim$270 P1 nodes) is even better than the solution obtained uniformly refining two times the initial mesh (u_2) which have a number of nodes, and then a computational cost, about four times greater.

In conclusion we can say that all the numerical tests show that mesh adaption is a very reliable tool for numerical simulation of shallow water steady flows. Both the error indicators used produce numerical results that are strongly improved with respect to a uniform mesh,

with only a minor increase in computational effort. The mesh refinement technique is almost decoupled from the numerical integration aspects and can thus be easily introduced also in codes that have not been originally designed in an adaptive perspective. Last but not least, the initial mesh generation does not require any a priori knowledge of the flowfield, as any sufficiently regular background grid is automatically refined to an almost optimal one.
Although other similar encouraging results have also been obtained applying this procedure to a test case of unsteady shallow water flow (not presented in this paper), further tests must be made before we can draw more general conclusions about the applicability of the above illustrated tool.

Acknowledgments
This research has been supported by the Sardinia Regional Authorities and by ENEL Ricerca, Polo Idraulico.

References

[1] D. Ambrosi, S. Corti, V. Pennati, and F. Saleri. Numerical simulation of unsteady flow at Po river delta. *J. of Hydraulic Engineering*, 122(12), 1996.

[2] C. Johnson. *Numerical solution of partial differential equations by the finite element method.* Cambridge University Press, 1987.

[3] R. Lohner. Finite element methods in CFD: grid generation, adaptivity and parallelization. In *Unstructured grids methods for advection dominated flows.* AGARD-R-787, 1992.

[4] V. Rudiger. *A Review of A Posteriori Error Estimation and Adaptive Mesh Refinement Techniques.* Wiley Teubner, 1996.

[5] R.A. Walters and E.J. Barragy. Comparison of H and P finite element approximations of the shallow water model. *Int. J. Numer. Meth. Fluids*, 24:61–79, 1997.

[6] O.C. Zienkiewikz and R.L. Taylor. *The finite element method.* Mc Graw–Hill, 1989.